Partial Differential Equations in Applied Mathematics 18 (2026) 101356

Contents lists available at ScienceDirect

Partial Differential Equations in Applied Mathematics

journal homepage: www.elsevier.com/locate/padiff

Simulation of density-dependence subdiffusion in chemotaxis

Akram Al-Sabbagh [a,*], Omar Al-Tameemi [a], Ruaa Wana [b], Salih Rashid Majeed [c], Jabir Alshehabi Al-Ani [d]

[a] Department of Mathematics and Computer Applications, College of Sciences, Al-Nahrain University, Jadriya Baghdad, Iraq
[b] Studies Planning and Follow-Up Directorate, Ministry of Higher Education and Scientific Research, Baghdad, Iraq
[c] SEAST, Canadian University, Dubai Dubai, UAE
[d] Department of Computer and Data Science, Business School, York St John University, York, UK

ARTICLE INFO

Keywords:
Anomalous subiffusion
Chemotaxis
Monte Carlo simulation

ABSTRACT

This paper presents a nonlinear, non-Markovian model of subdiffusive transport influenced by a chemotactic gradient affecting cellular mobility. In the model, both the stochastic waiting time and the escape rate are modulated by the chemotactic gradient. We derive the subdiffusive fractional master equation, examine its diffusive limit, and implement Monte Carlo simulations to analyse particle transport under varying chemotactic conditions. Simulation results show that, in the absence of chemotaxis, particles exhibit symmetric subdiffusion consistent with the standard continuous time random walk behaviour. A constant chemotactic gradient has little effect on particle distribution, whereas spatially varying gradients-linear or quadratic-produce pronounced effects. Specifically, particles drift away from regions with high chemotactic intensity and tend to aggregate in areas of minimal chemotactic influence, with the strongest aggregation observed under quadratic gradients. These findings highlight the significant role of spatially dependent chemotaxis in shaping anomalous subdiffusive transport dynamics.

1. Introduction

Cells, bacteria, and various other microscopic organisms exhibit random movement within their environment; this motility is essential for numerous biological phenomena, including wound healing and embryonic development,[1] agglomeration of bacteria into multicellular formations,[2] and various additional physiological mechanisms.[3]

Generally, this random movement is referred to as a *taxis*, derived from the Greek word for "arrange".[4] Taxis refers to a cell's directional movement in response to external stimuli. The alteration in the trajectory of the random movement pattern is a consequence of the reaction to these external stimuli.[4] Taxis can be formulated in several types exhibited by cells (or microorganisms), including haptotaxis (directed motility or cellular expansion), aerotaxis (movement in reaction to molecular oxygen), geotaxis (movement affected by gravitational forces), and chemotaxis[5] which we study in this work.

The chemotaxis can be defined as the oriented movement of cells in response to a chemical gradient, towards higher concentrations of helpful substances or lower concentrations of toxins, indicating a favourable environment. This phenomenon may be classified as negative or positive chemotaxis (Fig. 1), contingent upon the direction of movement relative to the stimulus influencing the chemical gradient.[4]

Chemotaxis, like other forms of taxis, consists of two primary components. The initial factor involves an intricate network of signals, including variations in global stimulation or chemoattractant concentration.[4] Organisms detect, evaluate, and then respond to these signals. Bacteria can detect a diverse array of external signals from their environment.[6] The second element of taxis is the bodily reaction that corresponds to these stimuli. The reaction may include a genetic modification, indicative of evolutionary change if these creatures have been subjected to the same signal over an extended period,[6] or they may react by migrating towards or away from the signal's source.

The migration of cells in a chemotactic gradient is closely associated with the intensity of the gradient and is contingent upon the polarisation of the cell itself. It exhibits distinct behaviour on high slopes compared to moderate gradients. In pronounced gradients, cells discern the gradient's direction and actively respond by moving, albeit with little deviations, towards the chemoattractant source.[7] They utilise receptor occupancy on their surfaces to compare and identify areas of higher concentration; this phenomenon is referred to as directional sensing.[8]

* Corresponding author.
E-mail addresses: akram.alsabbagh@alumni.manchester.ac.uk (A. Al-Sabbagh), omar.ismael@nahrainuniv.edu.iq (O. Al-Tameemi), ruaawana@mohesr.edu.iq (R. Wana), salih.majeed@cud.ac.ae (S. Rashid Majeed), j.alshehabialani@yorksj.ac.uk (J. Alshehabi Al-Ani).

https://doi.org/10.1016/j.padiff.2026.101356
Received 12 August 2025; Received in revised form 19 March 2026; Accepted 20 March 2026
Available online 23 March 2026

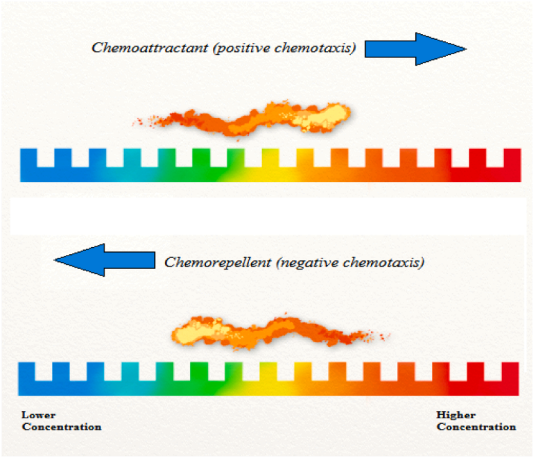

Fig. 1. The variation in organismal responses to chemical signals.[5]

Conversely, in a diminished gradient, such as in a uniform environment, cells alter their orientation randomly every second, resulting in an unguided random movement.

Chemotaxis and the random movement of cells have been extensively studied for an extended period.[9,10] A substantial body of experimental data elucidates critical aspects of the chemotaxis pathway, including the quantity and localisation of chemosensory proteins within the cell, among other details that facilitate the development of mathematical or computational models simulating cellular movement.[11] Nonetheless, despite the plethora of discoveries and elucidations offered by these models, several facets involving intricate nonlinear interactions remain ambiguous.[6]

This work aims to elucidate chemotaxis transport using continuous time random walk (CTRW) models utilising Monte Carlo simulation. CTRW has been significantly linked to different physical and biological processes, particularly in this area of transportation.[12] Many of these transition processes characterise the cell (particle) average mean squared displacement, $\langle x^2(t)\rangle \propto t^{\mu}$, resulting an anomalous behaviour with subdiffusive if $0 < \mu < 1$, or superdiffusive for $\mu > 1$.

Subdiffusion is essential for numerous chemotactic processes, including bacterial movement,[6] neutrophil infection response,[13] porous media,[14] and cell membranes,[15] among other topics.

Numerous studies in literature associate chemotaxis CTRW and address random walks characterised by run and trap dynamics (for further information, see Fedotov [16],Langlands and Henry [17]). A primary assumption in this literature is that chemotaxis alone impacts particles during the leap and does not effect particles when they remain stationary.

To elucidate this, we will provide the conventional CTRW model for the progression of subdiffusing entities that traverse randomly inside a one-dimensional lattice in a chemorepellent medium defined by a concentration gradient of $\Delta\mathtt{S}$. The generalised governing equation for this model is

$$\frac{\partial}{\partial t}\rho(x,t) = \mathtt{R}(x-a)\mathtt{i}(x-a,t) + \mathtt{L}(x+a)\mathtt{i}(x+a,t) - \mathtt{i}(x,t), \tag{1.1}$$

where $\rho(x,t)$ denotes the particle density at place x at time t, and $\mathtt{i}(x,t)$ represents the total escape rate, defined by

$$\mathtt{i}(x,t) = \frac{1}{\Gamma(1-\mu)\tau_0^{\mu}} D_t^{1-\mu}\rho(x,t). \tag{1.2}$$

This denotes the quantity of escaping particles from x. The integral escape rate $\mathtt{i}(x,t)$ in this case excludes chemotaxis, where the operator $D_t^{1-\mu}$ represents the Riemann-Liouville fractional derivative defined as,

$$D_t^{1-\mu} f(t) = \frac{1}{\Gamma(\mu)}\frac{d}{dt}\int_0^t \frac{f(\tau)}{(t-\tau)^{1-\mu}}d\tau. \tag{1.3}$$

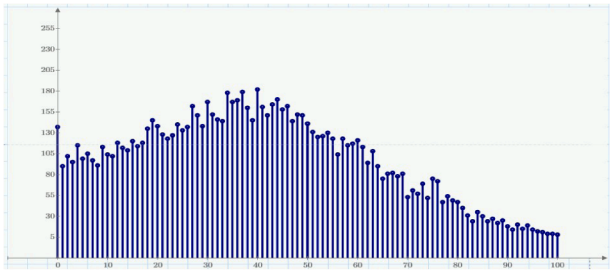

Fig. 2. The distribution of particles with no chemotactic effect.

Conversely, the probability of jumping to the right $\mathtt{R}(x)$ and to the left $\mathtt{L}(x)$ may be influenced by chemotactic gradients,

$$\mathtt{R}(x) = \frac{l}{2}\chi\Delta\mathtt{S}, \qquad \mathtt{L}(x) = \frac{l}{2}\chi\Delta\mathtt{S}. \tag{1.4}$$

The Eqs. (1.1), (1.2), and (1.4) culminate in the fractional Fokker-Planck equation (FFPE)

$$\frac{\partial\rho}{\partial t} = D_{\mu}\left[\frac{\partial^2}{\partial x^2} - \chi\frac{\partial}{\partial x}\Delta\mathtt{S}\right]D_t^{1-\mu}\rho. \tag{1.5}$$

In this context, D_{μ} and χ denote the diffusion and chemotactic coefficients, respectively.[12,18–20]

This study employs the nonlinear CTRW model for transport in biological systems characterised by chemotaxis and anomalous subdiffusion, as developed in.[5] We utilise the Monte Carlo method to simulate particle transport, incorporating the influence of chemotactic substances throughout the entire process, rather than solely during the jumping phase.

2. Chemotactic diffusion and fractional equation

In this section, the aim is to present the nonlinear model for subdiffusion of particles in chemotactic media. Assume a random walker moving, with step size of a, on a one-dimensional lattice, where chemotactic gradient consistently affects the particle at all time. The stochastic waiting time T_x is affected by the chemotactic gradient $\Delta\mathtt{S}$, alongside the jumping probability, as seen in model (1.1).

The model is fully derived in Al-Sabbagh [5] using the same mechanism used in Fedotov and Korabel [21] ,Al-Sabbagh [22]. Assuming the escape rates, which depend on the chemotactic gradient $\Delta\mathtt{S} = \mathtt{S}(x-a) - \mathtt{S}(x)$, are defined in Fedotov and Korabel [21] as

$$\begin{aligned}\mathtt{R}_c(x) &= \begin{cases} a\chi\Delta\mathtt{S}, & \Delta\mathtt{S} \geq 0,\\ 0, & \Delta\mathtt{S} < 0,\end{cases}\\ \mathtt{L}_c(x) &= \begin{cases} 0, & \Delta\mathtt{S} \geq 0,\\ -a\chi\Delta S, & \Delta\mathtt{S} < 0.\end{cases}\end{aligned} \tag{2.1}$$

The chemotactic gradient prevents the anomalous aggregation of particles at state x. In a diminished gradient, cells seem to migrate more slowly and remain at a single location for extended periods in the absence of chemotaxis.[23] This results in a significant alteration of the master equation that characterises the model. In addition, the nonlinear escape rate to the right, $\mathtt{R}_c(x,\tau)$, and the nonlinear escape rate to the left, $\mathtt{L}_c(x,\tau)$, from a point x, which incorporates both mean field density and chemotactic gradient, is expressed as

$$\begin{aligned}\mathtt{R}_c(x,\tau) &= \begin{cases} \mathtt{R}(x,\tau) + \alpha_{\mathtt{R}}(\rho) + a\chi\Delta\mathtt{S}, & \Delta\mathtt{S} \geq 0,\\ \mathtt{R}(x,\tau) + \alpha_{\mathtt{R}}(\rho), & \Delta\mathtt{S} < 0,\end{cases}\\ \mathtt{L}_c(x,\tau) &= \begin{cases} \mathtt{L}(x,\tau) + \alpha_{\mathtt{L}}(\rho), & \Delta\mathtt{S} \geq 0,\\ \mathtt{L}(x,\tau) + \alpha_{\mathtt{L}}(\rho) - a\chi\Delta\mathtt{S}, & \Delta\mathtt{S} < 0,\end{cases}\end{aligned} \tag{2.2}$$

where $\mathtt{R}$ and $\mathtt{L}$ are the standard escape rates and the additional $\alpha_{\mathtt{R}}(\rho)$ and $\alpha_{\mathtt{L}}(\rho)$ represent the non-linear escape rates to the right and left, with unspecified dependence to x and t. The escape rates (2.2) indicate that

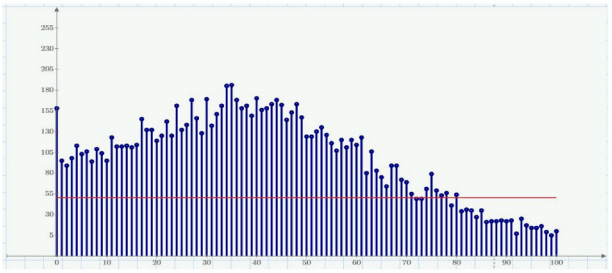

Fig. 3. The distribution of particles with constant chemotactic gradient.

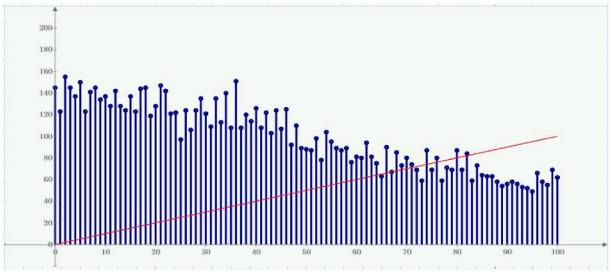

Fig. 4. The distribution of particles with steadily increasing chemotactic gradient.

the chemotactic gradient ΔS significantly influences the enhancement of subdiffusion to the right (when $\Delta S \geq 0$) or to the left (when $\Delta S < 0$). However, it has no effect on leaping to the left (if $\Delta S \geq 0$) or to the right (if $\Delta S < 0$); in other words, this model exhibits no symmetry regarding the chemotactic substance. Furthermore, while the escape rates remain contingent upon the residence period τ, the resultant model incorporating $\rho(x,t)$ is non-Markovian. Nonetheless, a Markovian model may be derived by proposing constant escape rates $\mathtt{R}$ and $\mathtt{L}$, together with a null chemotactic gradient $\Delta S = 0$. Furthermore, a normal FFPE may be acquired by assuming a zero chemotactic coefficient $\chi = 0$.

The literature has various efforts to formulate a modified fractional diffusion equation that incorporates chemotactic substances or other external forces and reactions.[12,21] Aside from the work of Fedotov and Korabel[21], these generalised master equations are not applicable to broader instances of anomalous diffusion, as chemotaxis may involve a physical interaction that connects the diffusion time scale with the effective chemorepellent time scale.

In order to formulate the generalised master equation incorporating the nonlinear escape rates in (2.2), we will employ the structured probability density function (PDF), $\xi(x,t,\tau)$ since the process is non-Markovian, and introduce the residence time τ as an auxiliary variable to the mean field density. This structured density indicates the quantity of particles that spent τ time in state x at time t.[1,24,25] The PDF adheres to the balancing equation.

$$\frac{\partial \xi}{\partial t} + \frac{\partial \xi}{\partial \tau} = -[\mathrm{R}_c(x,\tau) + \mathrm{L}_c(x,\tau)]\xi. \tag{2.3}$$

Initially, at time $t = 0$ and the residence time τ, the balance Eq. (2.3) satisfies the initial condition

$$\xi(x,0,\tau) = \rho_0(x)\delta(\tau), \tag{2.4}$$

where $\rho_0(x)$ denotes the initial density. The boundary condition at zero residence time is presented as follows:

$$\xi(x,t,0) = \int_0^t \mathrm{R}_c(x-a,\tau)\xi(x-a,t,\tau)d\tau + \int_0^t \mathrm{L}_c(x+a,\tau)\xi(x+a,t,\tau)d\tau. \tag{2.5}$$

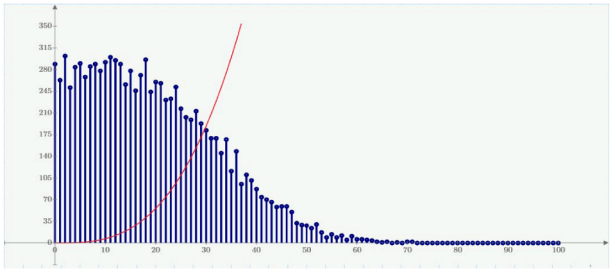

Fig. 5. The distribution of particles with exponential chemotactic gradient.

The primary objective now is to ascertain the general shape of the unstructured density

$$\rho(x,t) = \int_0^t \xi(x,t,\tau)d\tau. \tag{2.6}$$

This approach has been employed by numerous authors (see for instance[16,25–27]) to investigate the non-Markovian random walk, which has recently been recognised as a highly effective method for various nonlinear generalizations.[21,22,24,28–30] The generalised master equation is derived as fellows: (for the full derivation details see Al-Sabbagh [5])

$$\begin{aligned}
\frac{\partial \rho}{\partial t} &= e^{-\Phi(x,t)} \int_0^t \mathbb{K}_{\mathrm{R}}(x-a,t-\tau)e^{-a\chi|\Delta S(x-a)|\tau+\Phi(x,\tau)}\rho(x-a,\tau)d\tau \\
&\quad + \alpha_{\mathrm{R}}(\rho(x-a,t))\rho(x-a,t) \\
&\quad + e^{-\Phi(x,t)} \int_0^t \mathbb{K}_{\mathrm{L}}(x+a,t-\tau)e^{-a\chi|\Delta S(x+a)|\tau+\Phi(x,\tau)}\rho(x+a,\tau)d\tau \\
&\quad + \alpha_{\mathrm{L}}(\rho(x+a,t))\rho(x+a,t) \\
&\quad - e^{-\Phi(x,t)} \int_0^t \mathbb{K}(x,t-\tau)e^{-a\chi|\Delta S|\tau+\Phi(x,\tau)}\rho(x,\tau)d\tau - \alpha(\rho)\rho(x,t) \\
&\quad - a\chi|\Delta S|\rho(x,t) \\
&\quad + \begin{cases} a\chi\Delta S(x-a)\rho(x-a,t), & \Delta S \geq 0. \\ -a\chi\Delta S(x+a)\rho(x+a,t), & \Delta S < 0. \end{cases}
\end{aligned} \tag{2.7}$$

Presented herein, $\mathbb{K}_{\mathrm{R}}(x,t)$, $\mathbb{K}_{\mathrm{L}}(x,t)$, and $\mathbb{K}(x,t) = \mathbb{K}_{\mathrm{R}}(x,t) + \mathbb{K}_{\mathrm{L}}(x,t)$ are the dependent memory kernels defined in the Laplace domain as

$$\begin{aligned}
\hat{\mathbb{K}}_{\mathrm{R}}(x,s) &= \frac{\hat{\psi}_{\mathrm{R}}(x,s)}{\hat{\Psi}_{\gamma}(x,s)}, \\
\hat{\mathbb{K}}_{\mathrm{L}}(x,s) &= \frac{\hat{\psi}_{\mathrm{L}}(x,s)}{\hat{\Psi}_{\gamma}(x,s)}.
\end{aligned} \tag{2.8}$$

The master Eq. (2.7) includes the exponential factor $e^{-a\chi|\Delta S|\tau}$, which incorporates the chemotactic gradient ΔS, in addition to the exponential factor of the nonlinear rates.

At the same time, employing the Tauberian theorem, the memory kernels (2.8) may be asymptotically estimated in the Laplace domain as $s \to 0$ by

$$\hat{\mathbb{K}}_{\mathrm{R}}(x,s) = \frac{p_{\mathrm{R}}(x)s^{1-\mu(x)}}{g(x)}, \qquad \hat{\mathbb{K}}_{\mathrm{L}}(x,s) = \frac{p_{\mathrm{L}}(x)s^{1-\mu(x)}}{g(x)}, \tag{2.9}$$

where $g(x) = \Gamma(1-\mu(x))\tau_0^{\mu(x)}$. Given that $p_{\mathrm{R}}(x) + p_{\mathrm{L}}(x) = 1$. Subsequently, the collected memory kernel is

$$\hat{\mathbb{K}}(x,s) = \frac{s^{1-\mu(x)}}{g(x)}. \tag{2.10}$$

To obtain the macroscopic fractional diffusion equation, we consider the continuous diffusion limit of the lattice model. In this limit the lattice spacing (a) and the characteristic waiting-time scale (τ_0) tend to zero while maintaining the scaling relation

$$\frac{a^2}{\tau_0^{\mu}} \to D_{\mu},$$

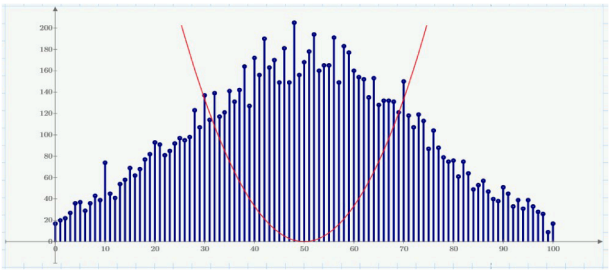

Fig. 6. The distribution of particles with quadratic chemotactic gradient.

where (D_μ) is the generalized subdiffusion coefficient. Under this hydrodynamic scaling, the density functions $(\rho(x \pm a, t))$ are expanded in a Taylor series around (x),

$$\rho(x \pm a, t) = \rho(x, t) \pm a\frac{\partial \rho}{\partial x} + \frac{a^2}{2}\frac{\partial^2 \rho}{\partial x^2} + O(a^3).$$

Substituting these expansions into the generalized master Eq. (2.7) and retaining terms up to order $(O(a^2))$ yields the continuum fractional diffusion equation. In this limit the memory kernels defined in (2.8)–(2.10) lead to the fractional time operator $(D_t^{1-\mu(x)})$, which characterizes the subdiffusive dynamics arising from the heavy-tailed waiting-time distribution. Consequently, the macroscopic transport equation takes the form given in:

$$\begin{aligned}\frac{\partial \rho}{\partial t} = -a^2\frac{\partial}{\partial x}\Bigg[&\frac{\beta \Delta S}{g(x)} e^{-a\chi|\Delta S|t-\Phi(x,t)} D_t^{1-\mu(x)}(\rho(x,t)e^{a\chi|\Delta S|t+\Phi(x,t)}) \\ &+\chi\rho(x,t)\Delta S + \kappa\frac{\partial \rho}{\partial x}\Bigg] \\ &+ \frac{a^2}{2}\frac{\partial^2}{\partial x^2}\mathrm{i}(x,t). \end{aligned} \tag{2.11}$$

Specifically, with identical jump probabilities $p_R(x) = p_L(x) = 1/2$, we obtain equivalent nonlinear rates $\alpha_R(\rho) = \alpha_L(\rho)$, resulting in identical escape rates $i_R(x,t) = i_L(x,t)$. Therefore, the fractional master equation may be expressed as

$$\frac{\partial \rho}{\partial t} = -a^2\chi\frac{\partial}{\partial x}\Big[\Delta S\rho(x,t)\Big] + \frac{a^2}{2}\frac{\partial^2}{\partial x^2}\mathrm{i}(x,t). \tag{2.12}$$

The fractional master Eq. (2.12) functions as a transition adaptor that alternates between transition modes based on the waiting duration of jumps. An intermediate subdiffusive mode is attained when $\tau_0/T_1 \ll 1$ and $a\chi|\Delta S|T_1 \ll 1$, whereas normal diffusion is observed when $a\chi|\Delta S|T_1 \gg 1$. We see that Eq. (2.12) lacks drift; rather, it incorporates the chemotactic gradient in both components of the right-hand side. Chemotaxis not only influences advection, as demonstrated in the standard model (1.5), but also incorporates a tempering parameter via the exponential component $e^{a\chi|\Delta S|t}$. The subsequent stage involves executing Monte Carlo method to simulate the final model in (2.11) as it is very complex to solve it numerically. However, the stationary form of (2.12) has been stationarily determined and numerical solution is presented for the stationary density in .[5]

3. Monte Carlo simulation

The Monte Carlo method provides a powerful computational framework for simulating stochastic processes, including anomalous transport phenomena such as subdiffusion. Standard simulation approaches employ a CTRW model. In the CTRW framework, subdiffusion emerges from a particle's trajectory governed by a heavy-tailed probability distribution of waiting times between successive spatial jumps.[12] The CTRW is a widely used Monte Carlo model for simulating subdiffusion. A particle's walk is defined by a sequence of jumps decoupled from a series of waiting times. To generate subdiffusive dynamics, the waiting times (τ) between jumps are drawn from a probability density function with a heavy, power-law tail. The occurrence of very long waiting times, which represent transient trapping events, is the microscopic origin of the macroscopic subdiffusive behavior. The simulation for an ensemble of particles involves iteratively drawing waiting times and jump lengths from their respective distributions to construct trajectories, from which observables like the MSD are calculated.[31]

In this work, the Monte Carlo method is run to simulate the subdiffusion of particles in a chemotactic media. The particles move on a one dimensional lattice $[0, 100]$, having three options: keep their position, moving to the right, or moving to the left with step size of a and with reflecting boundaries at 0 and 100. Then, after moving T time, the position of each particle is reported and the final particles distribution is built. The Monte Carlo method is run as following:

Step (1) Generate the waiting time with Mittag-Leffler distribution

$$\tau = -\tau_0 \ln u_1 \left(\frac{\sin(\mu(x)\ \pi)}{\tan(\mu(x)\ \pi\ u_2)} - \cos(\mu(x)\ \pi)\right)^{1/\mu(x)},$$

where u_1 and u_2 are two uniform (0,1) random numbers and τ_0 is the scale parameter.[32]

Step (2) After waiting time is over, the particle jumps either to the right or left x to $x+1$ or $x-1$ with probabilities $a(x,\tau,\rho)$ and $b(x,\tau,\rho)$.[5]

Step (3) Repeat Step (1) and Step (2) for $T = 10^3$ times.

Step (4) Note the particle's location at time T.

Step (5) Repeat all the steps for $\omega = 10^5$ particles, and note the locations of all of them to build up a histogram of the particle's distribution over the interval $[0, 100]$. Reflecting boundary conditions are imposed at (x=0) and (x=100), ensuring that particles reaching the boundaries remain within the computational domain.

4. Results and discussion

The results of Monte Carlo simulation are presented in (Figs. 2–6). First of all, Fig. 2 shows the distribution of 10^4 particles where there is no chemotactic gradient affecting the random walk. This result is shown in Al-Sabbagh [5],Falconer et al. [24]. In Fig. 3, the particles are affected with a constant level of chemotactic gradient. Since there is no difference in chemotactical level at each position, one can notice that there is no effect on the distribution of the particles. On the other hand, Fig. 4 shows the effect of the chemical gradient on the particles. Particles show a slow drift toward regions with lower chemotactic concentration, as expected under an increasing chemotactic gradient. However, the drift is still slow and there is no aggregation. However, in regions where the chemotactic gradient increases exponentially, particle diffusion is enhanced, as shown in Fig. 5, this results in particle aggregation in areas where the chemotactic influence is weakest. Fig. 6 clearly demonstrates this behaviour, particles preferentially avoid regions of high chemotactic gradient, resulting in aggregation at locations where the chemotactic effect is weakest.

5. Conclusions

This paper investigates a nonlinear, non-Markovian random walk model in which chemotaxis influences particle motion continuously during both the jumping and trapping phases. The generalised master Eq. (2.7), incorporating the exponential factor associated with the chemotactic gradient together with nonlinear escape rates, was presented. These components demonstrate how chemotaxis can reduce long trapping times and modify the effective transport dynamics. In contrast to classical fractional diffusion models, the resulting equation includes the chemotactic gradient in both the drift and diffusion terms.

The main contribution of this work is the implementation of a Monte Carlo simulation framework to study the nonlinear subdiffusion model described by Eq. (2.11). This approach enables the stochastic simulation of particle trajectories governed by density-dependent escape rates and chemotactic effects acting throughout the transport process. By simulating a large ensemble of particles, the method provides a numerical validation and physical interpretation of the theoretical fractional transport model.

The simulation results reveal key features of the transport dynamics. In the absence of chemotaxis, particles exhibit symmetric subdiffusive behaviour consistent with the classical continuous time random walk framework. When a constant chemotactic gradient is introduced, the particle distribution remains largely unchanged due to the uniform influence across the spatial domain. However, spatially varying chemotactic gradients produce significant changes in the transport dynamics. In particular, particles tend to drift away from regions with strong chemotactic intensity and accumulate in areas where the chemotactic influence is weaker. This aggregation effect becomes especially pronounced when the gradient varies quadratically.

Overall, these findings highlight the important role of spatially dependent chemotaxis in shaping anomalous subdiffusive transport and demonstrate the usefulness of Monte Carlo simulations for analysing complex nonlinear fractional models such as Eq. (2.11).

Data availability

No data was used for the research described in the article.

Declaration of competing interest

The authors declare that they have no known competing financial interests or personal relationships that could have appeared to influence the work reported in this paper.

Acknowledgements

The authors are very grateful to Prof. Sergei Fedotov for his great help and support. The authors would also like to thank the anonymous reviewers for their valuable comments and suggestions, which have significantly improved the quality and clarity of this manuscript.

References

1. Fedotov S, Ivanov AO, Zubarev AY, et al. Non-homogeneous random walks, subdiffusive migration of cells and anomalous chemotaxis. *Math Model Nat Phenom* 2013, 8(02):28–43. https://doi.org/10.1051/mmnp/20138203
2. Kay RR, Langridge P, Traynor D, Hoeller O, Changing directions in the study of chemotaxis, In: *Nat Rev Molecul Cell Biol* 2008;9(6):455. https://doi.org/10.1038/nrm2419
3. Ridley A, Schwartz MA, Burridge K, Firtel R, Ginsberg M, Borisy G, et al. Cell migration: integrating signals from front to back. English 2003.
4. Othmer HG, Stevens A. Aggregation, blowup, and collapse: the ABC's of taxis in reinforced random walks. *SIAM J Appl Math* 1997;57(4):1044–1081. https://doi.org/10.1137/S0036139995288976
5. Al-Sabbagh A, Nonlinear Models of Subdiffusive Transport with Chemotaxis and Adhesion, Ph.D thesis, The University of Manchester, 2016.
6. Wadhams GH, Armitage JP. Making sense of it all: bacterial chemotaxis. *Nat Rev Mol Cell Biol* 2004;5(12):1024–1037. https://doi.org/10.1038/nrm1524
7. Swanson J, Taylor D. Local and spatially coordinated movements in Dictyostelium discoideum amoebae during chemotaxis. *Cell* 1982;28(2):255.
8. Devreotes P, Janetopoulos C. Eukaryotic chemotaxis: distinctions between directional sensing and polarization. *J Biol Chem* 2003;278(23):20445–20448. https://doi.org/10.1074/jbc.R300010200
9. Ma M, Ou C, Wang Z, et al. Stationary solutions of a volume-filling chemotaxis model with logistic growth and their stability. *SIAM J Appl Math* 2012;72(3):740–766. https://doi.org/10.1137/110843964
10. Hillen T, Painter KJ. A user's guide to PDE models for chemotaxis. *J Math Biol* 2008;58(1–2):183–217. https://doi.org/10.1007/s00285-008-0201-3
11. Levin MD, Morton-Firth CJ, Abouhamad WN, Bourret RB, Bray D. Origins of individual swimming behavior in bacteria. *Biophys J* 1998;74(1):175–181. https://doi.org/10.1016/S0006-3495(98)77777-X
12. Metzler R, Klafter J. The random walk's guide to anomalous diffusion: a fractional dynamics approach. *Phys Rep* 2000;339(1):1–77. https://doi.org/10.1016/S0370-1573(00)00070-3
13. Van Haastert P, Devreotes PN, Chemotaxis: signalling the way forward, *Nat Rev Mol Cell Biol* 2004;5(8):626. https://doi.org/10.1038/nrm1435
14. Drazer G, Zanette DH. Experimental evidence of power-law trapping-time distributions in porous media. *Phys Rev E, Statist Phys, Plasma, Fluid Relate Interdiscipl Top* 1999;60(5 Pt B):5858–5864.
15. Saxton MJ, Jacobson K. Single-particle tracking: applications to membrane dynamics. *Annu Rev Biophys Biomol Struct* 1997;26:373–399.
16. Fedotov S. Subdiffusion, chemotaxis, and anomalous aggregation. *Phys Rev E* 2011;83(2):021110. https://doi.org/10.1103/PhysRevE.83.021110
17. Langlands TAM, Henry BI. Fractional chemotaxis diffusion equations. *Phys Rev E* 2010;81(5):051102. https://doi.org/10.1103/PhysRevE.81.051102
18. Metzler R, Klafter J, Barkai E. Anomalous diffusion and relaxation close to thermal equilibrium: a fractional Fokker-Planck equation approach. *Phys Rev Lett* 1999;82(18):3563–3567.
19. Barkai E, Metzler R, Klafter J, et al. From continuous time random walks to the fractional Fokker-Planck equation. *Phys Rev E* 2000;61(1):132–138. https://doi.org/10.1103/PhysRevE.61.132
20. Metzler R, Barkai E, Klafter J. Deriving fractional Fokker-Planck equations from a generalised master equation In: *Europhys Lett (EPL)* 1999;46(4):431–436. https://doi.org/10.1209/epl/i1999-00279-7
21. Fedotov S, Korabel N. Subdiffusion in an external potential: anomalous effects hiding behind normal behavior. *Phys Rev E* 2015;91(4):042112. https://doi.org/10.1103/PhysRevE.91.042112
22. Al-Sabbagh A. Subdiffusion of particles with a nonlinear interaction and cell-cell adhesion. *J Comput Theoret Transp* 2021;50(1):52–66. https://doi.org/10.1080/23324309.2020.1840395
23. Takeda K, Sasaki A, Ha H, Seung H, Firtel R. Role of phosphatidylinositol 3-kinases in chemotaxis in dictyostelium. *J Biol Chem* 2007;282(16):11874–11884.
24. Falconer S, Al-Sabbagh A, Fedotov S. Nonlinear tempering of subdiffusion with chemotaxis, volume filling, and adhesion. *Math Model Nat Phenom* 2015;10(3): 48–60. https://doi.org/10.1051/mmnp/201510305
25. Mendez V, Fedotov S, Horsthemke W. Reaction-Transport Systems: Mesoscopic Foundations, Fronts, and Spatial Instabilities. Springer; 2010. ISBN 978-3-642-11443-4.
26. Fedotov S, Falconer S. Subdiffusive master equation with space-dependent anomalous exponent and structural instability. *Phys Rev E, Statist, Nonlin Soft Matter Phys* 2012;85 (3 Pt 1):031132.
27. Yadav A, Horsthemke W. Kinetic equations for reaction-subdiffusion systems: derivation and stability analysis. *Phys Rev E* 2006;74(6): 066118. https://doi.org/10.1103/PhysRevE.74.066118
28. Fedotov S. Nonlinear subdiffusive fractional equations and the aggregation phenomenon. *Phys Rev E* 2013;88(3):032104. https://doi.org/10.1103/PhysRevE.88.032104
29. Fedotov S, Falconer S. Nonlinear degradation-enhanced transport of morphogens performing subdiffusion. *Phys Rev E* 2014;89(1): 012107. https://doi.org/10.1103/PhysRevE.89.012107
30. Straka P, Fedotov S. Transport equations for subdiffusion with nonlinear particle interaction. *J Theor Biol* 2015;366:71–83. https://doi.org/10.1016/j.jtbi.2014.11.012
31. Metropolis N, Ulam S. The monte carlo method In: *J Am Statist Assoc* 1949; 44:335–341. https://doi.org/10.1080/01621459.1949.10483310
32. Fulger D, Scalas E, Germano G. Monte carlo simulation of uncoupled continuous-time random walks yielding a stochastic solution of the space-time fractional diffusion equation. *Phys Rev E* 2008;77:021122. https://doi.org/10.1103/PhysRevE.77.021122